

International Journal of Nanoscience
Vol. 20, No. 5 (2021) 2150049 (13 pages)
© World Scientific Publishing Company
DOI: 10.1142/S0219581X21500496



Preparation of Gentamicin Sulfate Nanoparticles using Eudragit RS-100 and Evaluation of Their Physicochemical Properties

Ladan Nejati*, Nader Shakiba Maram* and Amanollah Zarei Ahmady^{†,‡}

**Nanotechnology Research Center*

*Ahvaz Jundishapur University of Medical Sciences
Ahvaz, Iran*

†Marine Pharmaceutical Sciences Research Center

*Ahvaz Jundishapur University of Medical Sciences
Ahvaz, Iran*

‡zarei-a@ajums.ac.ir

Received 15 May 2021

Accepted 9 November 2021

Published

Improving permeability and absorption of drugs are critical research challenges in pharmaceutical science. Gentamicin sulfate is an aminoglycoside antibiotic, which is very active against gram-negative bacteria; however, it has very poor bioavailability. This study aimed to prepare gentamicin nanoparticles with the intention of increased bioavailability. Accordingly, Eudragit RS-100 nanoparticles loaded with gentamicin sulfate were prepared by the double emulsification and solvent evaporation method, a proper technique for encapsulating hydrophilic molecules. Nanoparticles' suspensions with polymer to drug ratios of 1:1 (F_a) and 2:1 (F_b) were prepared, lyophilized and evaluated for their production yield, physicochemical properties and morphology. The mean particle size was 195.67 nm and 228 nm for F_a and F_b , respectively. The formulations' loading efficiencies were relatively high (85.73 for F_a and 85.20 for F_b). The nanoparticles' surface charge (+40.5 mV) was sufficient to inhibit their aggregation and facilitate the nanoparticles' absorption through the gastrointestinal tract. The results of differential scanning calorimetry (DSC) and Fourier transform infrared spectroscopy (FT-IR) revealed that drug and polymer stabilized each other by physical interactions between their functional groups. Both formulations presented an initial burst drug release of nearly 20% after 30 min in phosphate buffer (pH = 7.4). After 24 h, F_b did not release the drug completely, while F_a released the whole drug. Overall, nanoparticles with proper characteristics were obtained. This study puts forward the necessity of conducting further research in order to explore the intestinal absorption of these nanoparticles and the possibility of being utilized for oral administration of gentamicin sulfate.

Keywords: Eudragit RS-100; double emulsion; gentamicin; nanoparticles.

[‡]Corresponding author.

L. Nejati, N. S. Maram & A. Z. Ahmady

1. Introduction

Gentamicin is a member of aminoglycoside antibiotics with a small molecule and molecular weight of 477.603 g/mol. By binding to the ribosome, gentamicin inhibits protein synthesis in bacteria. The drug penetrates the cell membrane of oxygen-dependent bacteria and therefore has little effect on absolute anaerobes.¹ Gentamicin is used to treat many bacterial infections, like bone infection, endocarditis, pelvic inflammatory disease (PID), meningitis, pneumonia, urinary tract infection (UTI) and sepsis.² Owing to high water solubility and low permeability, gentamicin is categorized in class (III) of the biopharmaceutical classification system (BCS).³ Due to the negligible oral bioavailability of gentamicin sulfate, it is supplied as topical and parenteral dosage forms.

Nanoparticles are defined as colloidal solid particles with a size of less than 100 nm.⁴ Nanoparticles contain a wide range of materials, including polymers, metal oxides, nanotubes, liposomes and micelles. The three main factors that differentiate the nanoparticles of a material from its usual form are the increase in the surface-to-volume ratio of nanoparticles, the dimensions of the nanoparticles and the quantum effect. Due to these unique properties, the use of nanoparticles in a wide range of industries and even food and pharmaceutical products is increasing today. A remarkable advantage of nanoparticles is that they provide acceptable loading efficiency without disrupting drug activity by chemical interactions.⁵ Some researchers suggest that nanoparticles may increase the bioavailability of peptide and protein drugs by the following mechanisms: Reducing enzymatic degradation in the gastrointestinal tract, enhancing particle interactions with the site of absorption and direct entry into the bloodstream through the intestinal mucosa.⁶ Nanoencapsulation methods for hydrophilic molecules like peptides and proteins have some restrictions, such as the type of solvent, temperature and pressure used. Double emulsification and solvent evaporation is a suitable technique for encapsulation of hydrophilic molecules and significant encapsulation efficiencies are achievable for such molecules.⁷

Eudragit polymers are widely used to prepare conventional and novel oral dosage forms and can improve the oral bioavailability of poorly absorbed drugs.^{8,9} Eudragit RS-100 is an ester of acrylic and methacrylic acid with the structure of poly(ethyl

acrylate, methyl-methacrylate and negative-ammonioethyl methacrylate).¹⁰ This nonbiodegradable, low permeable and time-dependent polymer is regularly used in oral dosage forms and can improve their bioavailability.¹¹ The positively charged moieties of quaternary ammonium groups (4.5–6.8%) in the Eudragit RS-100 structure facilitate its interaction with tissues, as cell membranes possess a negative charge. This can utilize the gastrointestinal absorption of drugs.¹² Loveymi *et al.* improved vancomycin hydrochloride bioavailability by preparing Eudragit RS-100 nanoparticles using the double emulsification and solvent evaporation method.¹³ Momoh *et al.* improved the oral bioavailability of diclofenac sodium and reduced its gastrointestinal side effects by making RS-100 and RL-100 Eudragit microspheres.¹⁴

Double emulsion (W/O/W) is used to control the gradual release of hydrophilic drugs due to the presence of an oily layer that acts as a liquid membrane. In some cases, double emulsion can also be used as an internal reservoir to entrap the drug substance from the continuously diluted outer phase to the inner space. Gentamicin seems to be compatible with this method due to its numerous amino and hydroxyl groups and high hydrophilic properties.¹⁵

Double emulsions have been shown to have high interfacial and wide interfacial regions that provide thermodynamic stability. In these emulsions, changes in the viscosity of the immiscible phase or the thickness of this layer can be involved in the transfer of materials. One of the advantages of this method is its ease of production. To solve the basic problems of production, stirring of the immiscible phase must be minimized. Stirring affects the dispersion of droplets in the environment. One of the disadvantages of these emulsions is their instability or poor stability.¹⁶

One of the limitations of gentamicin is the short half-life of this drug (about 2 h), which can be overcome by nanoparticles.¹⁷

So far, gentamicin sulfate nanoparticles have been studied in various aspects. Pan *et al.* prepared calcium carbonate nanoparticles loaded with gentamicin sulfate and enhanced gentamicin antibacterial activity.¹⁸ Mazur *et al.* reported that gentamicin–silver nanoparticles significantly increased gentamicin efficacy and exhibited bactericidal activity against multidrug-resistant biofilm-forming *Staphylococcus epidermidis*.¹⁹ Posadowska *et al.* encapsulated gentamicin sulfate

in poly(lactide-co-glycolide) (PLGA) nanoparticles for topical drug therapy in osteomyelitis.²⁰

Due to simple administration and patient comfort, the oral route is the preferred way of drug delivery.²¹ Some studies aimed to improve gentamicin sulfate oral bioavailability. For instance, Akhtar *et al.* prepared gentamicin-PLGA nanoparticles, which were surfaced modified with chitosan. The preparation method was double emulsion and the authors reported that their nanoparticles had the potential for oral absorption of gentamicin sulfate.²² Despite the wide application of Eudragit polymers in oral dosage forms and their potential for enhancing poor oral bioavailability of drugs, the use of Eudragit nanoparticles for improving gentamicin sulfate oral bioavailability have not been studied in the literature. Therefore, the main objective of this study was to prepare gentamicin sulfate biocompatible nanoparticles using Eudragit RS-100. Considering the hydrophilicity of gentamicin sulfate, double emulsification and solvent evaporation was selected as the preparation method. Nanoparticles' physicochemical properties were characterized to evaluate the capability of this approach for providing desirable nanoparticles with the potential of being further investigated in terms of their oral bioavailability. Based on the low removal of nanoparticles and their high absorption by cells, can gentamicin be converted to nanoparticles to improve its absorption? In addition, are these nanoparticles suitable in terms of physicochemical properties? This study is a pilot study to increase the stability and bioavailability of gentamicin for effective oral administration.

2. Materials

Gentamicin sulfate was a gift from Exir pharmaceuticals, Iran. Eudragit RS-100 was provided by Evonic Co., Germany. Polyvinyl alcohol (PVA) (130KD), dichloromethane, glacial hydrochloric acid, monobasic potassium phosphate and potassium chloride were received from Samchun Co., South Korea. Sodium hydroxide (Merck, Germany) and the dialysis bag with the cut-off of 12KD (Sigma-Aldrich Co, Germany) were purchased from the indicated sources.

3. Methods

3.1. Preparation of nanoparticles

Nanoparticles were prepared using double emulsification and solvent evaporation technique. 50 mg of

gentamicin sulfate was dissolved in 5 ml of water to make the internal aqueous phase. 50 mg of Eudragit RS-100 for F_a (1:1) and 100 mg for F_b (1:2) was dissolved in 15 ml of dichloromethane to make the internal organic phase. The aqueous solution was dropped into the organic phase within 20 s intervals under homogenizer (Heidolph, SilentCrusher M, Germany) at 22000 rpm and homogenized for an extra 3 min after the last drop. While homogenizing at 22000 rpm, this primary water in oil (W_1/O) emulsion was added by a syringe, gently to 25 ml of PVA 0.2% as a stabilizer in an ice bath. Homogenization was continued for 3 min after complete addition. To evaporate the organic solvent, the prepared $W_1/O/W_2$ double emulsion was stirred at 1000 rpm on a magnetic-heater-stirrer (CAT, M6.2, Germany) for 3 h at room temperature. Finally, the nanoparticles' suspension was centrifuged (VigioN, 3000, South Korea) for 20 min with a rate of 20000 rpm at 25°C. The supernatant was used for loading efficiency studies. The sediment was washed with distilled water and lyophilized by a freeze-drier device (CHRIST, Alpha 1-2 LDplus, Germany) for subsequent assessments. Independent *T*-test with *P*-value (≤ 0.05) was used to define the significant difference between the formulations.

3.2. Characterization of nanoparticles

3.2.1. Production yield

Following freeze-drying of the nanoparticles, the formulations' production yield was calculated by Eq. (1). The test was repeated three times for each formulation,

Production yield

$$= \frac{\text{weight of freeze dried nanoparticles (mg)}}{\text{weight of drug} + \text{weight of polymer (mg)}} \times 100. \quad (1)$$

3.2.2. Loading efficiency

10 ml of the supernatant, containing unloaded drug was inserted into the 12 kD dialysis bag (Sigma, United States). The dialysis bag was put in 20 ml of PVA solution (0.2%) for 1 h on a magnetic-stirrer (CAT, M6.2, Germany) at 50 rpm. After the equilibration of solutions, PVA was let at room temperature for five days, until its volume reduced to 5 ml and the ultraviolet (UV) absorption of unloaded drug solution became detectable by a

L. Nejati, N. S. Maram & A. Z. Ahmady

UV/visible spectrophotometer (Cecil England, CE2501, England). The measurement was run at gentamicin sulfate maximum wavelength ($\lambda_{\max} = 247 \text{ nm}$). The entrapment efficiency (EE%) was calculated using the following equation:

$$\text{EE\%} = \frac{\text{weight of drug in the formulation (mg)} - \text{weight of drug supernatant (mg)}}{\text{weight of drug in the formulation (mg)}} \times 100. \quad (2)$$

3.2.3. Particle size analysis

To examine the formulations' particle size, 0.5 ml of the nanoparticles' suspension was exposed to a laser particle size analyzer (qudix, Scatterscope I, South Korea). The mean particle size and standard deviation were calculated for three samples of each formulation and the polydispersity index (PDI) was obtained via the following equation:

$$\text{P.D.I} = \frac{\text{SD}^2}{\text{mean}^2}. \quad (3)$$

To evaluate the size distribution pattern, the under-size cumulative percentage of the particles' number versus particle size was assessed as log-probability and arithmetic-probability plots in Excel 2013. The model with a greater correlation coefficient (R^2) was determined as the distribution model.

3.2.4. Fourier transform infrared spectroscopy

To reveal probable interactions between the drug and polymer, infrared spectroscopy of the formulations and pure drug was carried out by an IR spectroscope equipment (vortex 70, Bruker, Germany) using a potassium bromide (KBr) disk over a range of 4000–500 cm^{-1} .

3.2.5. Differential scanning calorimetry

To evaluate the samples' physical properties and investigate possible interactions between components of the formulations, differential scanning calorimetry (DSC) studies were accomplished. Accordingly, 5 mg of the formulations and pure drug were analyzed by a DSC equipment (Mettler Toledo, Switzerland) at the rate of 10°C/min and temperature range between 25–350°C.

3.2.6. Zeta potential analysis

To determine the surface charge of the nanoparticles, a Zetasizer (Malvern, ZEN3600, United

Kingdom) device was occupied. Nanoparticles of F_a were considered as the sample formulation and were suspended in distilled water (pH = 7.0) at 25°C before measurement.

3.2.7. Scanning electron microscopy

As the sample formulation, F_b suspension was dripped on an aluminum sheet and dried at room temperature. After coating with gold, imaging was carried by a scanning electron microscope (TESCAN, MIRA3TESCAN-XMU, Czech Republic) to evaluate the nanoparticles' morphologic characteristics.

3.2.8. Dissolution study in phosphate buffer

The *in vitro* release profile of gentamicin sulfate from the polymeric nanoparticles was studied via dialysis bag diffusion technique under sink condition for both formulations. The dialysis bag retained the nanoparticles and allowed immediate drug diffusion into the recipient compartment.

80 mg of each formulation was added to the dialysis bag (12 kD), containing 10 ml of phosphate buffer (pH = 7.4) to stimulate the intestinal medium. The dialysis bag was put into 20 ml of phosphate buffer (pH = 7.4) placed in a preheated water bath at $37 \pm 1^\circ\text{C}$ on a magnetic-heater-stirrer at the rate of 50 rpm. After 0.5, 1, 2, 4, 6, 8, 24 h, the dialysis bag was removed from the Becher and put in 20 ml of fresh buffer. The sample volumes were reduced to 5 ml employing a rotary device (Heidolph, 4EF63CX-4, Germany) at 40°C, so that their UV absorption could be measured by the spectrophotometer. The solutions' UV absorption was measured at 247 nm. The test was repeated three times for each formulation.

3.2.9. Dissolution study in hydrochloric acid

To study the release profile of gentamicin sulfate in gastric acid, 50 mg of each formulation and 10 ml of HCl (pH = 1.2), which stimulated the gastric acid, were added to the dialysis bag. The dialysis bag was put into 20 ml of HCl (pH = 1.2) stirring at 50 rpm in a preheated water bath at $37 \pm 1^\circ\text{C}$ on a magnetic-heater-stirrer. The dialysis bag was taken out from the beaker after 1 and 2 h and put in 20 ml of fresh buffer. To make their UV spectrophotometry possible, the samples' volume was reduced to 5 ml by rotary (at 40°C). The solutions' UV absorption

was measured at 247 nm. The test was repeated three times for each formulation.

3.2.10. Dissolution kinetic

The *in vitro* release profiles were fitted to various kinetic models (Higuchi, first-order, zero-order, Peppas, Hixson Crowell, square root of mass, three-second root of mass, Weibull, linear probability and log-probability) in order to realize the drug release mechanism.²³ The slope of the respective plots was used to find out the velocity constants. The obtained data were also put into the Korsmeyer–Peppas model to determine the n value, which indicates the drug release mechanism.

3.2.11. Drug susceptibility to acidic medium

To assess the stability of gentamicin sulfate in acidic media similar to stomach pH, the drug concentration of 11.13 mg/ml was made in HCl (pH = 1.2). At the time of preparation and after 1 h, UV absorption of the prepared solution was analyzed by the spectrophotometer at 247 nm. The concentration of gentamicin sulfate was calculated using the calibration curve equation.

4. Results and Discussion

4.1. Production yield

The production yield of the formulations is indicated in Table 1. F_b production yield (90.20%) was significantly more than F_a (66.71%), with the P -value of 0.007.

The total amount of drug and polymer in F_b was more than that of F_a . This can be due to the higher viscosity of F_b compared to F_a , which when the amount of polymer increases during the production of particles, the viscosity of the solution increases, and this causes the drug to be more surrounded by the polymer and thus the amount of the production

yield increases. Subsequently, the ratio of waste substances to production material was smaller in F_b . Consequently, the presented ratio in Eq. (1) and the production yield of F_b were higher than F_a . On the other hand, with increasing viscosity, the diffusion rate of methylene chloride solvent decreases and this increases the formation time of nanoparticles and increases the production yield.

4.2. Loading efficiency

The loading efficiency was calculated to be 85.73% and 85.20% for F_a and F_b , respectively. Both formulations possessed acceptable loading efficiencies without significant difference. Eudragit RS-100 contains a small percentage of quaternary ammonium groups in its structure, which makes the polymer surface thick. This restricts the leakage of the entrapped drug into the surrounding medium, during the entrapment process and the mentioned issue causes the amount of loading efficiency to increase.²⁴

4.3. Particle size

The mean particle size and PDI of both formulations are demonstrated in Table 1. Both formulations were of a submicron size, and the difference between their particle sizes was not significant (P -value = 0.51). Barzegar–Jalal reported the same result regarding the sizes of nanoparticles containing 1:1 and 3:1 ratios of Eudragit RS-100: drug.²⁵ By increasing the amount of polymer in F_b , the polymer film forms quickly around the drug, preventing the drug from entering the methylene chloride solvent, which results in particle size increase. On the other hand, increasing the amount of polymer enhances the solution viscosity, which reduces the dispersion of the dispersed phase into smaller particles and increases the particle size. Furthermore, the greater amount of polymer declines the migration of emulsion droplets from the organic phase. This increases the probability of colloid formation leading to particle size growth.

The PDI for both formulations was less than 0.2, which is considered to be acceptable for polymer-based nanoparticles.²⁶ A significant difference between the formulations' PDIs was not observed (P -value > 0.80). Uniform size distribution of the nanoparticles is helpful, since it leads to predictable pharmacokinetics.

Table 1. The mean production yield, loading efficiency, mean particle size and PDI of F_a and F_b .

Formulation	Production yield (%) \pm SD ^c	Particle size (nm) \pm SD	PDI ^d \pm SD
F_a^a	66.71 \pm 4.87	195.67 \pm 67.50	0.135 \pm 0.068
F_b^b	90.20 \pm 5.57	228 \pm 37.75	0.141 \pm 0.071

Notes: ^aPolymer to drug ratio of 1:1, ^bpolymer to drug ratio of 2:1, ^cstandard deviation and ^dpolydispersity index.

L. Nejati, N. S. Maram & A. Z. Ahmady

4.4. Zeta potential

Zeta potential was measured +40.5 mV for F_a , as the sample formulation (Fig. 1). It belongs to the positive surface charge of Eudragit RS-100 and the negative charge of gentamicin sulfate; encapsulation of the drug into the polymer was confirmed and as demonstrated by SEM imaging, an even polymeric coat was constructed.²⁷ The zeta potential of F_b is greater than the formulation F_a , and this is due to the higher amount of positively charged polymer.

The surface charge of the nanoparticles influences their distribution and absorption into the cells. Owing to the negative charge of cell membranes, there is the most electrostatic desire for the positively charged particles. Additionally, suspended particles may be absorbed faster than the coagulated ones.²⁸ The measured zeta potential was sufficient for providing good stability and inhibiting the aggregation of the nanoparticles.²⁹ Moreover, the structural moieties with positive charge facilitate Eudragit RS-100 interaction with tissues. This can utilize the gastrointestinal absorption of drugs with low oral bioavailability.^{30–32} According to the

charge of living cells, the probability of absorption of F_b is greater than that of F_a .

4.5. Scanning electron microscopy

The signals used by SEM result from the interaction of the electron beam with the atoms at different depths inside the sample, which provide the image. SEM images (Fig. 2) demonstrated that the nanoparticles had a spherical and relatively uniform surface, which makes it possible to predict their pharmacokinetic parameters, including absorption, distribution, metabolism and excretion in the body.

4.6. Fourier transform infrared spectroscopy

The Fourier transform infrared spectroscopy (FT-IR) spectra are shown in Figs. 3–6. The peaks at 3617 cm^{-1} and 3742 cm^{-1} were observed in the nanoparticles' IR spectra, which probably were related to the shifting of gentamicin hydroxyl and amine stretching peaks at 3431 cm^{-1} and

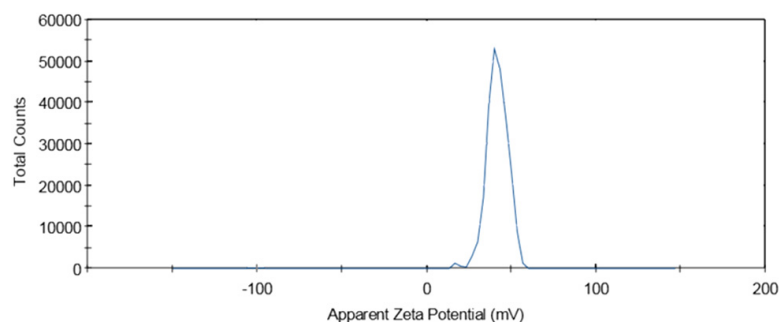


Fig. 1. Zeta potential of F_a (polymer: drug = 1:1) as the sample formulation.

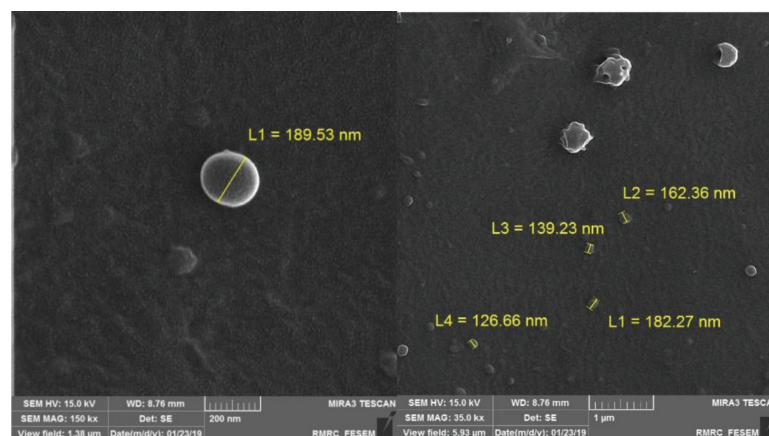


Fig. 2. SEM images of F_b (polymer: drug = 2:1).

Preparation of Gentamicin Sulfate Nanoparticles using Eudragit RS-100

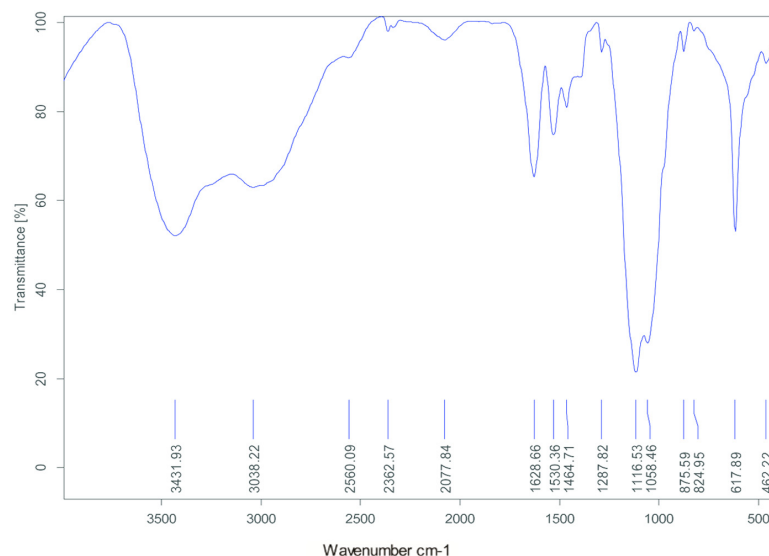


Fig. 3. FT-IR spectrum of gentamicin sulfate powder.

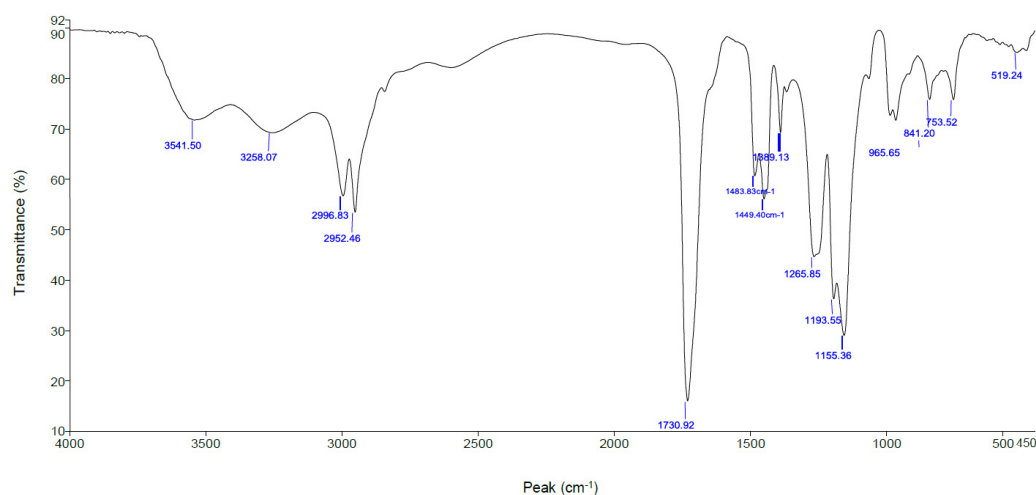


Fig. 4. FT-IR spectrum of Eudragit RS-100.³³

3038 cm^{-1} . It could be due to inhibition of gentamicin sulfate intramolecular hydrogen bindings, which led to enforcement of -NH and -OH bonds. Moreover, the stretching peak at 1733 cm^{-1} belonged to the Eudragit RS-100 carbonyl group, shifted to a higher wavelength because of increased polarity and strengthening of the carbon-oxygen bond. Most likely, the hydroxyl groups of gentamicin sulfate attracted the steric oxygen electrons of Eudragit RS-100 through hydrogen bindings. According to the analysis of drug, polymer and nanoparticles' IR spectra, physical interactions between the drug and polymer were demonstrated, which reduced the intensity of the mentioned peaks in the gentamicin sulfate spectrum. Adibkia *et al.*

also reported the hydrogen bindings between naproxen and Eudragit RS-100 functional groups in their prepared nanoparticles.³⁰ In the FTIR spectrum of the nanoparticles, the peaks of the functional groups in the drug are visible, indicating that no chemical reaction has taken place between the drug and the polymer and that the drug has been physically loaded.

4.7. Differential scanning calorimetry

The results of the DSC analysis are shown in Figs. 7–10. As indicated, a large and sharp peak was observed between $150\text{--}160^\circ\text{C}$ in the thermograms of gentamicin sulfate and both formulations,

L. Nejati, N. S. Maram & A. Z. Ahmady

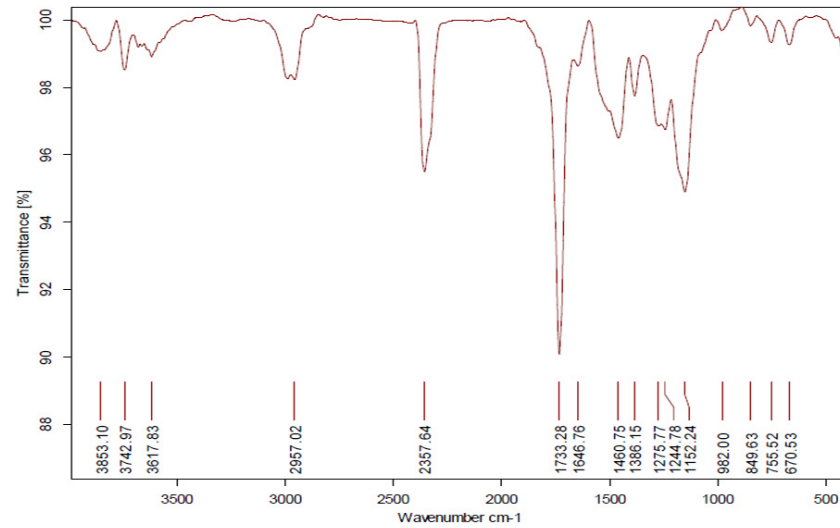


Fig. 5. FT-IR spectrum of F_a (polymer: drug = 1:1).

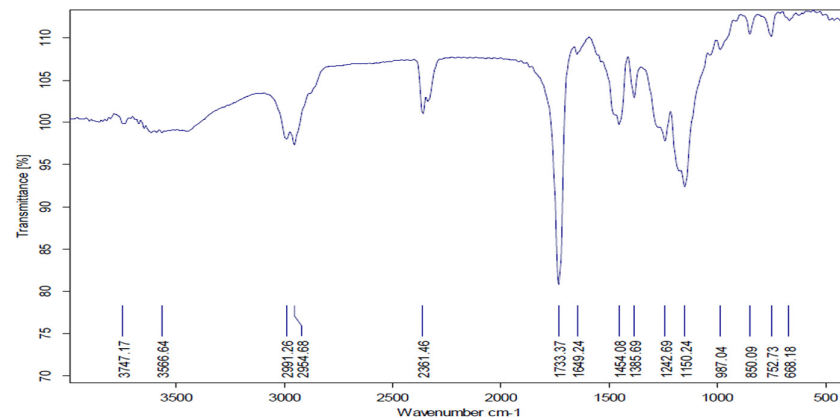


Fig. 6. FT-IR spectrum of F_b (polymer: drug = 2:1).

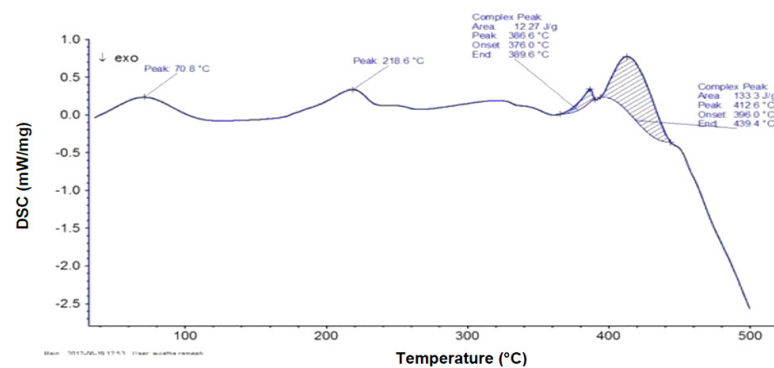


Fig. 7. DSC thermogram of Eudragit RS-100.³³

demonstrating the presence of drug in the nanoparticles without any chemical changes. The presence of polymer in the formulations made this peak wider in comparison with the pure drug. Accordingly, the higher ratio of Eudragit in F_b led to a

wider peak than F_a and this is due to the high polymer content, which has many amorphous properties. In addition, fewer amount of gentamicin in F_b compared to F_a in a 5 mg sample caused the peak height to be shorter in F_b . In regard to

Preparation of Gentamicin Sulfate Nanoparticles using Eudragit RS-100

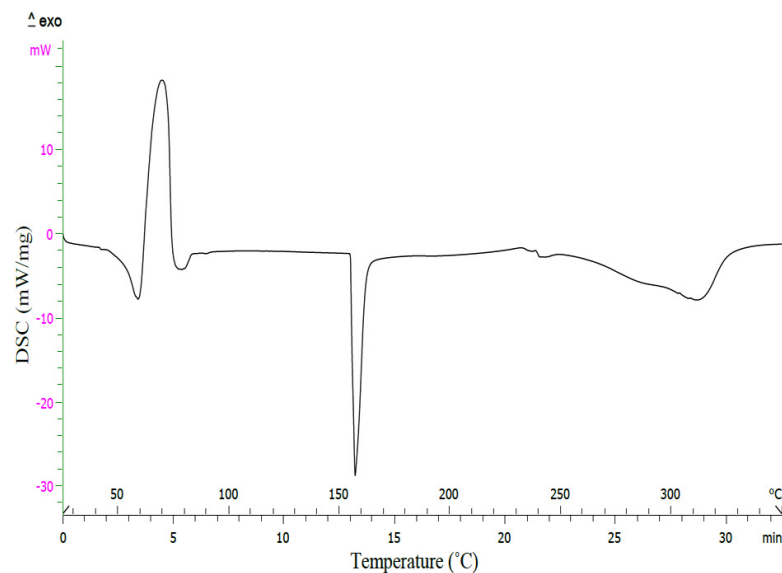
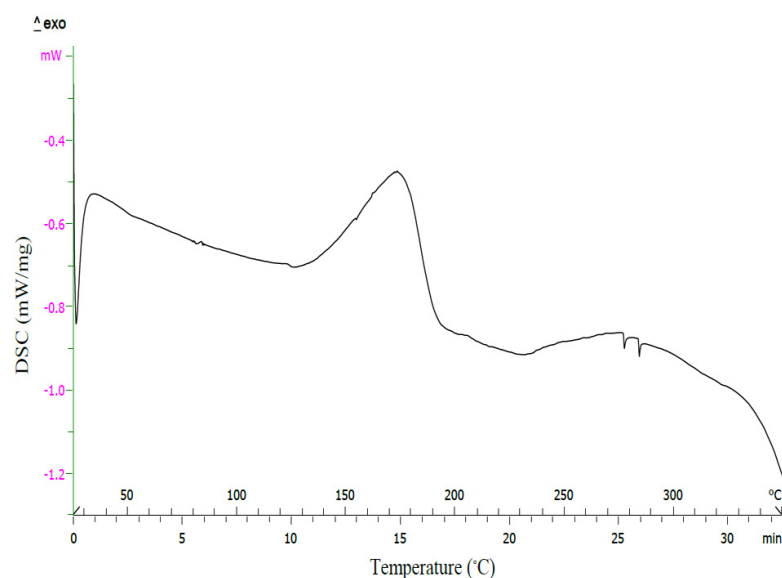


Fig. 8. DSC thermogram of gentamicin sulfate powder.

Fig. 9. DSC thermogram of F_a (polymer: drug = 1:1).

nanoparticles, the mentioned peak was shorter than pure drug, as well. Most probably, the decline of intensity of the later peak in gentamicin thermogram was related to solubilization of the drug in the polymeric matrix or the heating induced solid-state interactions.³⁰ Almost all fluctuations of gentamicin sulfate thermogram were also observed in the formulations, which confirmed the existence of the undamaged drug in the nanoparticles.

Based on DSC, physical interactions between gentamicin sulfate and Eudragit RS-100 stabilized the drug in nanoparticles' structure. The physical

nature of the interactions was concluded from FT-IR spectra of the nanoparticles. On the other hand, changing the polymer to drug ratio demonstrated that these interactions considerably enhanced Eudragit RS-100 thermal stability. The percentage of drug thermal decomposition was reduced in F_b . This indicated gentamicin thermal stability in the presence of Eudragit RS-100 and therefore the stability of the prepared nanoparticles. On the nanoparticles of DSC thermograms, peaks related to gentamicin are visible, indicating no chemical reaction between the drug and polymer.

L. Nejati, N. S. Maram & A. Z. Ahmady

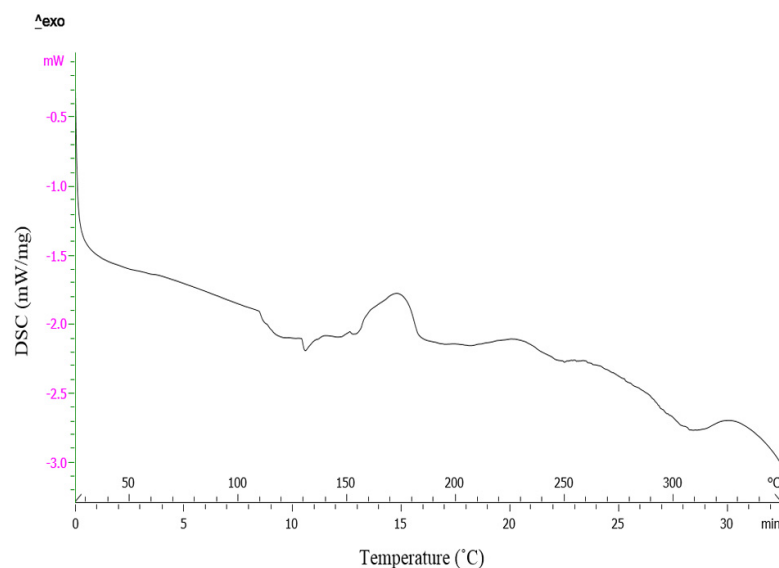


Fig. 10. DSC thermogram of F_b (polymer: drug = 2:1).

4.8. Dissolution profile in phosphate buffer

Both formulations had an initial burst release of about 20% of the drug after 30 min (Fig. 11). Burst release commonly occurs in the release profile of almost all microspheres made by solvent evaporation technique.³⁴ It is supposed to be due to the erosion of the surface of the particles and releasing of the drug situated near the surface and adsorbed by electrostatic forces.³⁵

Erosion of the nanoparticles' wall, dissolution and diffusion of the drug into the dissolution medium seems to be the primary mechanism for sustained drug release from the nanoparticles following the initial burst release.³⁰ Burst releasing of the drug can improve its penetration, while sustained releasing delivers the drug to the absorption site during a long time.³⁶

At the end of the test, about 50% of gentamicin sulfate was released from F_b . Mady also reported the incomplete ibuprofen release from Eudragit RS-100 microspheres.³⁴ Results of various studies have shown that the incomplete drug release is regular with solvent evaporation technique. In correspondence to the literature, this could be either the result of drug-polymer interactions or the retarding property of the polymer. It was also proposed to be related to the penetration of the sink medium into the microspheres or great drug solubility in the polymer matrix.³⁷ Similar to gentamicin sulfate, Eudragit RS-100 has hydrophilic molecules³⁸ and this may facilitate gentamicin sulfate solubility in the polymer matrix, which could be confirmed by drug-polymer interactions explained in DSC and FT-IR analysis.

Despite F_b , the whole drug was released from F_a after 24 h. The amount of the polymeric $-\text{NH}_3$

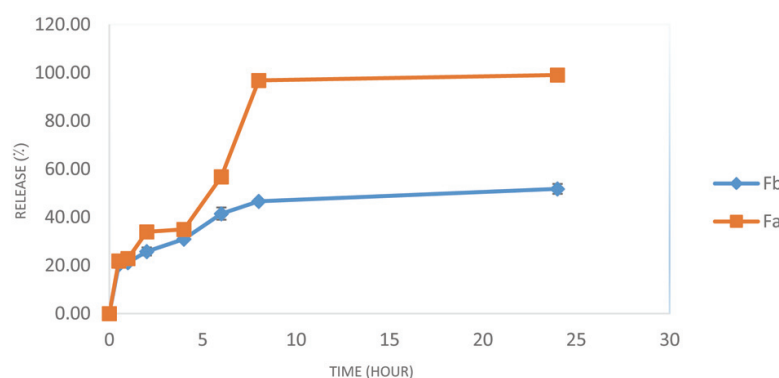


Fig. 11. Release profiles of F_a (polymer: drug = 1:1) and F_b (polymer: drug = 2:1) in phosphate buffer at pH = 7.4.

Preparation of Gentamicin Sulfate Nanoparticles using Eudragit RS-100

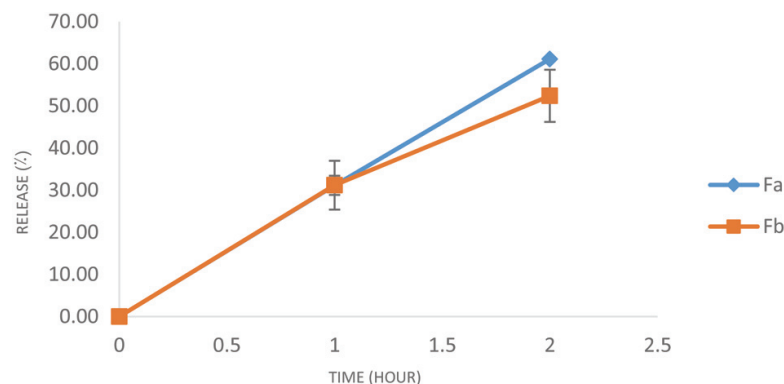


Fig. 12. The release profiles of F_a (polymer: drug = 1:1) and F_b (polymer: drug = 2:1) in HCl at pH = 1.2.

groups that physically interact with the drug $-OH$ groups is more significant in F_b compared to F_a . These hydrogen bonding interactions, as explained by DSC and FT-IR analysis, could probably lessen the swelling of Eudragit RS-100 following the absorption of the dissolution medium. This reduces the drug diffusion from the gel layer formed after water absorption.³⁹ The relation between swelling properties of the excipients and drug release profile was discussed in various studies.⁴⁰ The higher amount of polymer in F_b makes the nanoparticle wall more coherent compared to F_a , making it

difficult for the dissolution liquid to penetrate the particles and dissolve the drug.⁴¹

4.9. Dissolution profile in hydrochloric acid

Both formulations released about 30% of gentamicin sulfate within the first hour in HCl (Fig. 12). At the end of 2 h, about 50% and 60% of the drug was released from F_b and F_a , respectively. The difference between drug release percentage from F_a and F_b in HCl was not significant (P -value = 0.075). More

Table 2. Fitting parameters of the *in vitro* release data to various release kinetic models for nanoparticles.

Formulation	Order	RSQ ^a	Slope	Intercept	MPE ^b %	K ^c	
F_a^d	Zero order	0.685	0.041	0.2634	2927286.447	0.041	
	First order	0.7250	-0.2396	-0.2803	2718084.14	-0.2396	
	Second order	0.8222	6.5271	-5.1812	13772827.77	6.5271	
	Higuchi	0.8547	0.2327	0.0387	511433.1706	0.2327	
	Peppas (Power Low)	0.9174	1.4031	-2.7798	92.5762	4.0677	
	Hixson-Crowell	0.7149	0.0377	0.0986	2973661.989	0.0377	
	Square root of mass	0.7108	0.0416	0.1450	2989439.781	0.0416	
	Three-seconds root of mass	0.7050	0.0425	0.1878	2979131.498	0.0425	
	Weibull	0.9558	1.5487	-2.2075	47.9883	0.2404	
	Linear probability	0.5287	0.2128	-1.3274	1024652.909	0.2128	
	Logarithmic probability	0.8858	0.7037	-0.2815	44.1904	0.7037	
	F_b^e	Zero order	0.5944	0.0164	0.2046	2558280.614	0.0164
		First order	0.6804	-0.025	-0.2362	2630084.642	-0.0249
Second order		0.7557	0.0394	0.2727	2679016.279	0.0394	
Higuchi		0.8537	0.1022	0.1018	1313133.413	0.1022	
Peppas (Power Low)		0.8976	1.3671	-2.9849	163.0286	3.9238	
Hixson-Crowell		0.6527	0.0072	0.0750	2608321.791	0.0072	
Square root of mass		0.6384	0.0101	0.1099	2596580.816	0.0101	
Three-seconds root of mass		0.6239	0.0125	0.1431	2584307.853	0.0125	
Weibull		0.9072	1.3989	-2.8098	82.3547	0.1342	
Linear probability		0.202	0.0887	-1.4777	872031.2755	0.0887	
Logarithmic probability		0.9583	0.4907	-1.067	58.8009	0.4907	

Notes: ^aRegression square, ^bminimum possible error, ^cconstant dissolution rate, ^dpolymer to drug ratio of 1:1 and ^epolymer to drug ratio of 2:1.

L. Nejati, N. S. Maram & A. Z. Ahmady

minor drug release from F_b compared to F_a at the end of two hours is due to more excellent protection of the drug by the polymer.

–OH groups, which can make hydrogen bindings with hydrochloric acid, causes gentamicin sulfate to be more soluble in HCl rather than phosphate buffer. This could result in more rapid drug dissolution and its faster release in acidic medium compared to phosphate buffer. According to the results of the drug sensitivity test to the acidic medium, it was shown that although gentamicin is released faster in HCl, it is resistant to this medium and is not destroyed during passing the stomach.

4.10. Dissolution kinetic

According to Table 2, a high correlation was observed for Weibull ($R^2 = 0.9558$) and logarithmic probability ($R^2 = 0.9583$) models for F_a and F_b , respectively. According to Fick's law, the initial fast drug release is controlled by the erosion of the nanoparticles' wall and drug diffusion rate. After the establishment of the sink and stable condition, the constant diffusion rate was observed. Because, after saturation of the dissolution medium, drug concentration has a minor effect on the release rate. The n value for nanoparticles was 1.4031 in F_a and 1.3671 in F_b , indicating that the mechanism of drug release was mainly controlled by polymer erosion and, to a lesser extent, diffusion.

4.11. Drug susceptibility to acidic medium

The drug UV absorption at the preparation time and after 1 h was measured as 1.970 and 1.902, respectively. In regard to the calibration curve equation, the drug concentration after 1 h was 10.75 mg/ml. Thus, the amount of drug damaged in HCl after 1 h was negligible. Therefore, it could be concluded that gentamicin sulfate keeps its structure in the stomach pH before reaching the duodenum.

5. Conclusions

This study investigated the application of Eudragit RS-100 for preparing biocompatible nanoparticles of gentamicin sulfate by double emulsification and solvent evaporation technique to decrease the drug elimination by phagocytic cells, improve its absorption and increase its oral bioavailability.

Because it has been proven that nanoparticles absorb better than ordinary particles and their elimination by body cells occurs less often, the findings demonstrated that this simple and low-cost approach could provide gentamicin sulfate nanoparticles with relatively appropriate physicochemical characteristics. This work puts forward the requirement of conducting further research to explore the intestinal absorption of these nanoparticles. The oral way will bring more convenience to patients and increase their compliance to drug therapy. Therefore, evaluating the nanoparticles' capability for being utilized as a drug delivery system for oral administration of gentamicin sulfate would be beneficial. According to the low dose of gentamicin and its inability to be absorbed orally and if a polymer is added to the preparation of nanoparticles, it seems that this drug is a good candidate for nanoparticulate. Also, the study of antibacterial activity of gentamicin sulfate nanoparticles compared to the pure drug would be desirable.

6. Declarations

6.1. Funding

This work was financially supported by a grant (N-9609) from the Vice Chancellor for Research Affairs of Ahvaz Jundishapur University of Medical Sciences. This paper is issued from the thesis of Ladan Nejati.

References

1. H. Mohanty, S. Pachpute and R. P. Yadav, *Folia Microbiol.* **66**, 1 (2021).
2. R. Dorati, A. DeTrizio, M. Spalla, R. Migliavacca, L. Pagani, S. Pisani, E. Chiesa, B. Conti, T. Modena and I. Genta, *Nanomaterials* **8**, 37 (2018).
3. N. A. Mondal, G. L. Devi, K. Shiva, M. Mahender and J. Sharma, *Int. J. Scientific Development and Research* **6**, 242 (2021).
4. N. Shakiba-Maram, O. K. Avarvand, N. Mohtasham and A. Z. Ahmady, *Int. J. Nanosci.* **20**, 2150022 (2021).
5. N. Faramarzi, J. Mohammadnejad, H. Jafary, A. Narmani, M. Koosha and B. Motlagh, *Int. J. Nanosci.* **19**, 2050002 (2020).
6. E. Mathiowitz, *Encyclopedia of Controlled Drug Delivery*, Vol. 2 (Wiley-Interscience, 1999).
7. J. Zhang, J. Wang, F. Qiao, Y. Liu, Y. Zhou, M. Li, M. Ai, Y. Yang, L. Sui and Z. Zhou, *Colloids Surf.*

Preparation of Gentamicin Sulfate Nanoparticles using Eudragit RS-100

- B. Biointerfaces* **199**, 111560 (2021), doi: 10.1016/j.colsurfb.2021.111560.
8. S. K. Jain, A. K. Jain and K. Rajpoot, *Curr. Drug Deliv.* **17**, 448 (2020).
 9. M. Naeem, M. Choi, J. Cao, Y. Lee, M. Ikram, S. Yoon, J. Lee, H. R. Moon, M.-S. Kim and Y. Jung, *Drug Des. Dev. Therapy* **9**, 3789 (2015).
 10. Z. Mkhize, P. S. Seboletswe, H. K. Paumo, P. K. Boniface and L. M. Katata-Seru, *Int. J. Nanosci.* **20**, 2150017 (2021).
 11. A. Obinu, G. Rassu, P. Giunchedi and E. Gavini, *Pharmaceutics* **13**, 670 (2021).
 12. Q. Q. Zhao, X. Y. Zhang, X. F. Tang and H. Qiao, *J. Drug Deliv. Sci. Technol.* **66**, 102777 (2021), doi: 10.1016/j.jddst.2021.102777.
 13. B. D. Loveymi, M. Jelvehgari, P. Zakeri-Milani and H. Valizadeh, *Adv. Pharm. Bull.* **2**, 43 (2012).
 14. M. Momoh, F. Kenechukwu, M. Adedokun, C. Odo and A. Attama, *Drug Deliv.* **21**, 193 (2014).
 15. H. Zhang, Y. Jin, C. Chi, G. Han, W. Jiang, Z. Wang, H. Cheng, C. Zhang, G. Wang and C. Sun, *Biomaterials* **273**, 120824 (2021).
 16. T. M. Ho, A. Razzaghi, A. Ramachandran and K. S. Mikkonen, *Adv. Colloid Interface Sci.* **299**, 102541 (2022).
 17. A. S. Ali, *Bull. Pharma. Sci. Ass.* **44**, 31 (2021).
 18. X. Pan, S. Chen, D. Li, W. Rao, Y. Zheng, Z. Yang, L. Li, X. Guan and Z. Chen, *Front. Chem.* **5**, 130 (2018).
 19. P. Mazur, I. Skiba-Kurek, P. Mrowiec, E. Karczewska and R. Drożdż, *Int. J. Nanomed.* **15**, 3551 (2020).
 20. U. Posadowska, M. Brzychczy-Włoch and E. Pamuła, *Acta Bioeng. Biomech.* **17**, 41 (2015).
 21. M. I. Teixeira, C. M. Lopes, M. H. Amaral and P. C. Costa, *Eur. J. Pharma. Biopharma.* **149**, 192 (2020), doi: 10.1016/j.ejpb.2020.01.005.
 22. B. Akhtar, F. Muhammad, B. Aslam, M. K. Saleemi and A. Sharif, *Int. J. Biol. Macromol.* **164**, 1493 (2020).
 23. K. Chakravarty and D. Dalal, *Int. J. Biomath.* **11**, 1850011 (2018).
 24. V. Lavanya, P. Rajeswari, M. Vidyavathi and R. Sureshkumar, *Int. J. Nanosci.* **19**, 1950036 (2020).
 25. M. Barzegar-Jalali, M. Alaei-Beirami, Y. Javadzadeh, G. Mohammadi, A. Hamidi, S. Andalib and K. Adibkia, *Powder Technol.* **219**, 211 (2012).
 26. M. Danaei, M. Dehghankhold, S. Ataei, F. Hasan-zadeh Davarani, R. Javanmard, A. Dokhani, S. Khorasani and M. Mozafari, *Pharmaceutics* **10**, 57 (2018).
 27. W. Zhang, X. Li, T. Ye, F. Chen, S. Yu, J. Chen, X. Yang, N. Yang, J. Zhang and J. Liu, *Int. J. Nanomed.* **9**, 4305 (2014).
 28. Z. He, X. Wang, Y. Luo, Y. Zhu, X. Lai, J. Shang, J. Chen and Q. Liao, *Chemosphere* **277**, 130327 (2021), doi: 10.1016/j.chemosphere.2021.130327.
 29. E. Trenkenschuh and W. Friess, *Int. J. Pharm.* **606**, 120932 (2021), doi: 10.1016/j.ijpharm.2021.120932.
 30. K. Adibkia, Y. Javadzadeh, S. Dastmalchi, G. Mohammadi, F. K. Niri and M. Alaei-Beirami, *Colloids Surf. B. Biointerfaces* **83**, 155 (2011).
 31. K. Dillen, J. Vandervoort, G. Van den Mooter and A. Ludwig, *Int. J. Pharm.* **314**, 72 (2006).
 32. R. Bodmeier and H. Chen, *J. Control. Release* **10**, 167 (1989).
 33. Y. D. Reddy, D. Dhachinamoorthi and K. C. Sekhar, *J. Chem. Pharm. Res.* **7**, 19 (2015).
 34. O. Mady, *MOJ Bioequiv. Bioavailab.* **4**, 193 (2017).
 35. L. Tan, Z. Liu, C. Zhou and L. Ding, *J. Nanoparticle Res.* **23**, 1 (2021).
 36. Z. Cao, X. Tang, Y. Zhang, T. Yin, J. Gou, Y. Wang and H. He, *Int. J. Pharm.* **607**, 121021 (2021), doi: 10.1016/j.ijpharm.2021.121021.
 37. R. Jeyanthi and K. P. Rao, *Int. J. Pharm.* **55**, 31 (1989).
 38. H. Batista, J. P. Freitas, A. Abrunheiro, T. Gonçalves, M. H. Gil, M. Figueiredo and P. Coimbra, *Int. J. Polymeric Mater. Polymeric Biomater.* **1** (2021).
 39. M. Tannous, F. Caldera, G. Hoti, U. Dianzani, R. Cavalli and F. Trotta, *Supramol. Drug Discov. Drug Deliv.* **2207**, 247 (2021).
 40. E. Kaffash, M. Abbaspour, H. A. Garekani, Z. Jahanian, F. Saremnejad and A. Akhgari, *Adv. Pharm. Bull.* **11**, 318 (2021).
 41. B. Nath, L. K. Nath and P. Kumar, *Acta Pol. Pharm.* **68**, 409 (2011).